

Smart Inspection Tools in robotized aircraft panels manufacturing

Andrea Bruni
Research for Innovation
Loccioni
Angeli di Rosora (AN),
Italy
a.bruni@loccioni.com

Enrico Concettoni
Research for Innovation
Loccioni
Angeli di Rosora (AN),
Italy
e.concettoni@loccioni.com

Cristina Cristalli
Research for Innovation
Loccioni
Angeli di Rosora (AN),
Italy
c.cristalli@loccioni.com

Matteo Nisi
Research for Innovation
Loccioni
Angeli di Rosora (AN),
Italy
m.nisi@loccioni.com

Abstract—This paper presents the Smart Inspection Tools developed for the robotic cell designed for fuselage panels manufacturing, in the LABOR project. This project has the objective to develop a small size, low-cost automatic cell for the drilling, fastening, sealing and inspection of fuselage panels for regional aircraft. This paper focuses on the development of the two Smart Inspection Tools used for referencing the robot with respect to the panel geometry and to check the quality of the manufactured holes. Different inspection technologies have been exploited to guarantee the strict project specifications. The paper presents the design of the developed tool and shows the experimental results of a prototypal versions.

Keywords—*Inspection tool, Vision system, Robotized Aircraft manufacturing, Countersink hole inspection, Fastener inspection*

I. INTRODUCTION

One of the most important challenges for the next aircraft assembly lines is the increase in the level of automation. There are several reasons to pursue such an objective as the high-quality standards allowed by automatized solutions or the high production rates and flexibility. These features are more and more important since aerospace production volumes have been increasing steadily over the last three years. For instance, Boeing Commercial Airplanes built more than 700 airliners in 2014 while about 650 in 2013 and 600 in 2012. Furthermore, the annual report by Airbus (year 2016) reveals a long backlog of 6.847 aircraft, with only 688 commercial aircraft delivered, representing about 10 years of production at current rates. Airbus projects a need for about 35,000 new passenger aircraft – valued at US\$5.3 trillion – over the next 20 years, based on its latest Global Market Forecast (GMF): “Growing Horizons” [1]. Overall, the total worldwide fleet of passenger and freighter aircraft will double by 2036 – with an estimated requirement for 24.810 new single-aisle aircraft, 8.690 new twin-aisle wide-bodies and 1.410 new very large aircraft [1]. For this reason, main aeronautic manufacturers are heavily investing in flexible systems to reduce costs, improve quality and boost productivity, mainly by adopting robots, Automated Guided Vehicles (AGV) and other technologies. Drilling, fastener insertion, riveting, sealing, coating and painting applications, in addition to material handling, are the most recurrent operations in aircraft assembly lines. The majority of these operations are performed by machines and big robots, i.e., high-cost rigid solutions [2-5], but still a high number of the drilling and riveting operations are performed by the operators. Therefore, it is clear that the automation of such operations would lead to great and immediate benefits to aircraft industry in terms of production rate. However, mainly because of safety motivations and government regulations, hard constraints are requested to be met, especially concerning the process tolerances.

The LABOR project [6] will approach the problem with a new concept based on Self-Adaptive Robotic Cell that combines:

- small/medium size robots to provide higher capability of adaptation and easy integration in shop floor already existing facilities as shown in [7-9],
- adaptive processing tools in order to perform in an automatic and adaptive way the different processing tasks,
- advanced vision systems in order to reference the robots and check the quality of the work performed, and distributed intelligence in order to build a more flexible solution.

In the aircraft manufacturing process, the state of the art for the inspection of holes and fasteners relies on manual mechanical instruments. Each measurement has its own gauge: height/depth gauge, chamfer gauge, grip length gauge, gap gauge, shape gage and many others that guarantee the required measurement accuracy. A first approach toward measurement automation can be the use of such probes on a robotic arm. However, the use of contact measurement system on the robot, as presented in [10], is not effective due to the difficult integration of manual probes on an automatic system and due to the reduced robot accuracy. A better approach is represented by non-contact measurement systems which allow a better integration on robot wrist, especially as regard vision measurement techniques. The measurement is usually performed in different positions to cover undercut, thus requiring the use of a robot to perform the task. High accuracy instrumentation is bulky and not really suitable to be integrated in a fast tool changer as in [11-12]. Better results can be obtained with non-contact inspection probes as represented in [13-15]. These solutions guarantee high accuracy but they are very expensive and not so rugged to be safely installed on an automatic process in an industrial environment. The most suitable solutions are thus represented by vision non-contact inspection techniques based on the use of 2D cameras and lighting systems as in [16-17]. However, solutions found in the state of art have still some limits because does not guarantee the required accuracy or they are focused on a specific and particular measurement losing in generality. The same limits have been found among commercial solutions. For example, [18] has tried to overcome these limitations by developing a series of instruments dedicated to online surface measurements for the aeronautic sector, but their line-up is limited to dent and rivet flushness measurement. For a complete measurement set, [19] has presented an instrument for diameter, countersink diameter, countersink depth, grip length and perpendicular measurement but this tool is designed to be hand held and cannot perform referencing tasks.

In conclusion, the constraints in the present applications impose a design for a tool specifically developed for the integration in an automatic process and suitable to be mounted on a robotic arm.

In this contest, the LABOR Smart Inspection Tools have been developed, with the aim of reducing costs, weights, and dimensions according to the small-scale robot integration but respecting at the same time the strict requirements of the aeronautical sector. In the following paragraphs firstly the specifications for the Smart Inspection Tools will be summarized. Then, the proposed inspection techniques will be presented and the developed tools will be described. Finally, experimental results conducted with Smart Inspection Tools prototypes will be presented and discussed.

II. PROJECT REQUIREMENTS

The panels that must be manufactured in the LABOR robotic cell are composed of a CFRP skin with frames and shear ties temporarily glued on the skin. The LABOR robotic cell must drill and fastener holes on the outer panel surface to obtain a definitive coupling. The Smart Inspection Tools developed in the LABOR project have three main objectives:

- O1: scan from the internal side of the panel the geometry of the substructure (frames and shear ties) in order to reposition and align the robot before drilling;
- O2: check the quality of the drilled holes in terms of absence of delamination (or burrs in case of metals) occurring at the joint interfaces or at the exit of the hole, the hole diameter, and countersink;
- O3: check the quality of the installed fasteners in terms of flushness and sleeve diameter and height.

In Fig. 1 the countersink hole parameters are highlighted and the fastener main components are depicted. In Fig. 2, Fig. 3 and Fig. 4 the fastener installations parameters are described. According to the project specifications, maximum acceptable limits for the parameters described above are summarized in TABLE I.

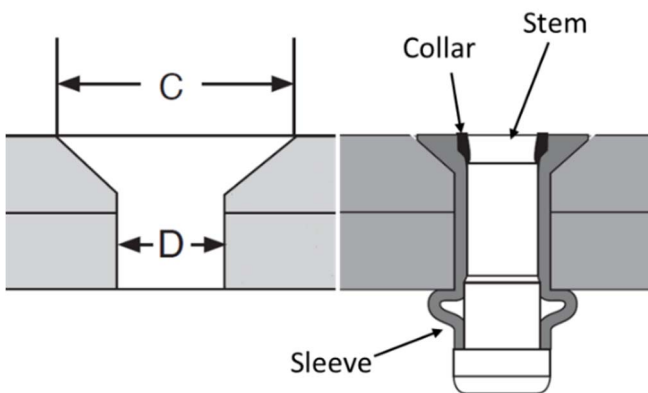


Fig. 1. Holes parameters and fasteners components

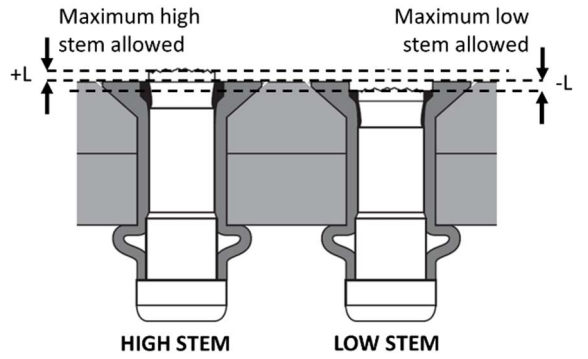


Fig. 2. Fastener Stem installation limits

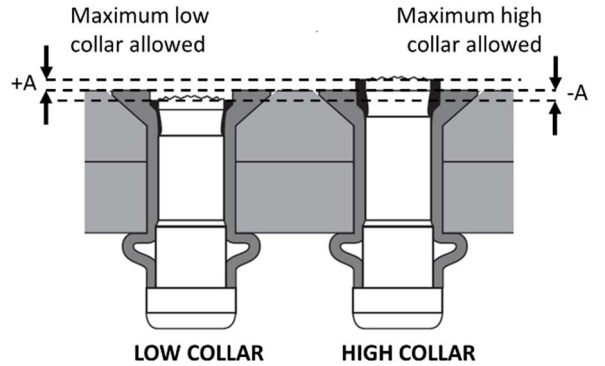


Fig. 3. Fastener Collar installation limits

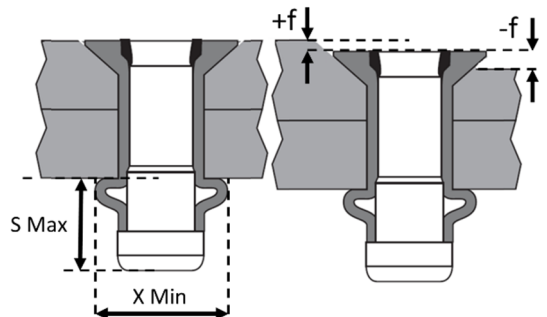


Fig. 4. Fastener Sleeve and Flushness installation limits

TABLE I. Hole dimensions and fastener installation parameter according to LABOR project specifications

Parameter	Value
Hole position tolerance	± 0.2 mm
Hole diameter tollerance (D)	[0 - 0.076] mm
Countersink diameter tolerance (C)	± 0.0635 mm
Flushness tolerance (f)	± 0.203 mm
Maximum Sleeve height (S Max)	5.9 mm
Minimum Sleeve diameter (X Min)	5.7 mm
Stem protrusion limits (C)	± 0.254
Collar protrusion limits (A)	± 0.4318

III. METHODOLOGY

The different required measurements are performed with two Smart Inspection Tools mainly for geometrical and weight constraints. The small/medium size robot has a limited payload, thus two smaller and lighter tools have been preferred with respect to a single bigger tool. Each tool exploits a different inspection technique and guarantees the required measurement performances as specified in [20]. The first tool (represented in Fig. 5) uses a 2D camera for measuring the hole diameter and the countersink diameter (O_2).

The tool is composed of the following parts:

- One Camera
- Telecentric Lens
- Diffusive ring light (blue 450nm)
- A band-pass filter centered on 450nm

Several lighting solutions with different wavelength have been tested mainly because the reflection of the CFRP countersink hole creates problems for a correct measurement of both diameters (hole and countersink). Spotlights due to a direct reflection of light source on the camera sensor cause the saturation of the image and reduce the quality of the diameter measurement. Thus, a different technique has been proposed based on a diffusive blue (450nm) ring light that significantly reduces the reflection thanks to a diffuser and a different incident light angle. The internal and external diameters are then measured through an edge detection analysis (Fig. 6). The measurement algorithm automatically finds the hole within the image, compares the measured diameters with the nominal tolerance defined in TABLE I and assess if the drilled hole can be accepted, otherwise requires the operator attendance. Finally, the 2D Smart Inspection Tool is mounted on an electric linear axis that allows adjusting the camera focus. Indeed, the robot position error can, affects the distance between the camera and the panel, thus causing errors in the diameter measurements. To correct this issue, autofocus techniques can be tested in order to adjust the camera distance by moving the linear axis and then improving the measuring accuracy.

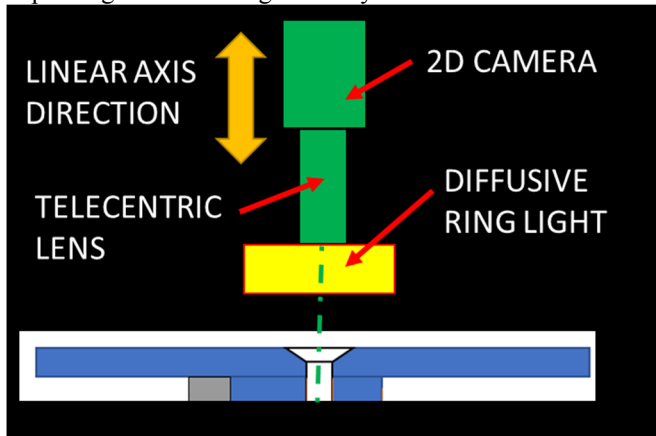


Fig. 5. 2D Smart Inspection Tool

The second Smart Inspection Tool is represented in Fig. 7; it measures the correct installation of the fastener and scans the internal panel surface for robot reference (O_1 and O_3). It

consists of a profilometer composed of a structured LED light pattern projector and two cameras to avoid undercuts [21].

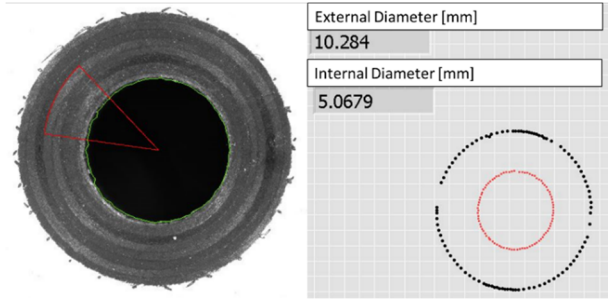


Fig. 6. Image acquired (left); Image elaboration (right)

The tool is composed of the following parts:

- Two cameras
- 35mm Lens
- A structured LED light pattern projector.

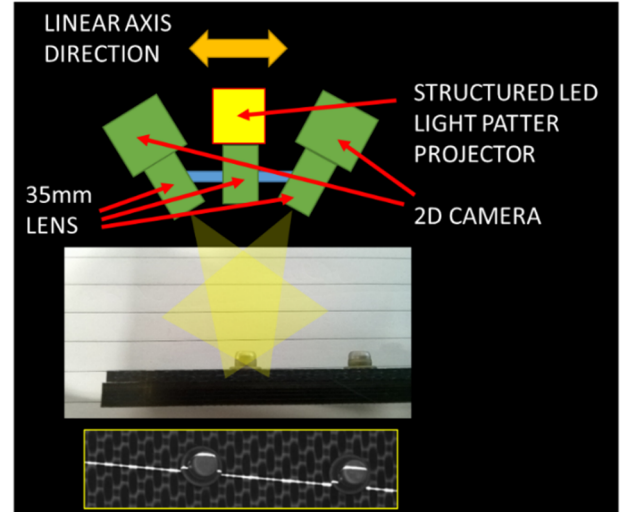


Fig. 7. 3D Smart Inspection Tool

The structured LED light projects on the target a 10 μm width line. The use of a blue LED source instead of a laser reduces speckle and increases accuracy. The two cameras extract the profiles (left and right) to ensure a complete view of the target even in case of one camera has undercut or occlusions. The 3D Smart Inspection Tool is mounted on an electric linear axis that allows translating the tool on a direction perpendicular to the projected line. At regular intervals, the tool extracts two profiles like the one represented in Fig. 8. All the profiles are then combined together allowing a 3D reconstruction (point cloud) of the scanned object (Fig. 9). Finally, the left and right point clouds (extract from the left and right cameras) are merged to obtain a complete reconstruction of the target object. The obtained point cloud contains a great number of information that can be elaborated to extract the required measurement by interpolating geometrical entities.

The proposed approach allows to increase the tool flexibility, the design is not specific for a particular measurement and several quantities can be extracted by analyzing the point cloud. In detail, for the purposes of the LABOR project, the 3D Smart Inspection Tool can be used to measure all the

required quantities on the fastener head and sleeve and to reconstruct the geometry of the internal panel surface.

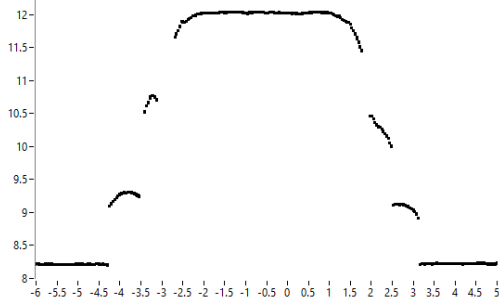


Fig. 8. Extracted profile

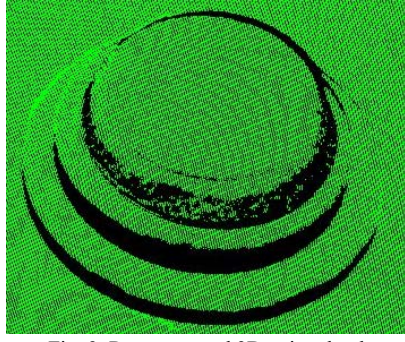


Fig. 9. Reconstructed 3D point cloud

The proposed Smart Inspection Tools, both for 2D and 3D inspection, satisfy the project requirements: small dimensions, lightweight, accurate measurements, and flexibility. In the following paragraph, a preliminary test on tool prototypes will be presented,

IV. RESULTS

In this paragraph, preliminary results of the measurements conducted with the Smart Inspection Tools prototypes are presented. In Fig. 10 a correct and incorrect installed fastener are represented for both the fastener head and sleeve. In Fig. 11 examples of extracted profiles are presented, while in Fig. 12 the point clouds of a corrected and uncorrected installer fastener head are compared.



Fig. 10. Correct installed and defected fastener head and sleeve

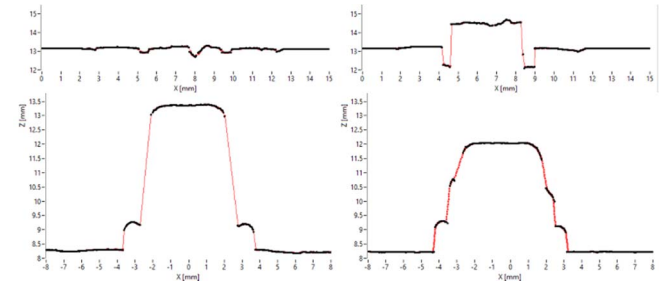


Fig. 11. Correct installed and defected fastener head and sleeve (profile)

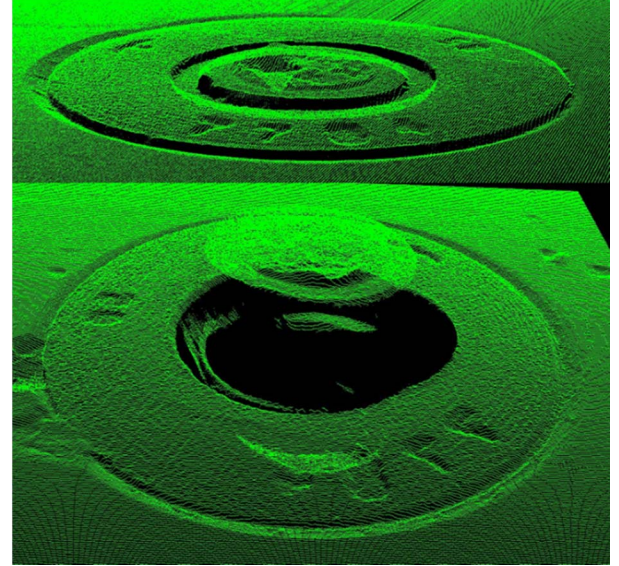


Fig. 12. Correct installed and defected fastener head (point cloud)

The profiles can thus be elaborated to extract the geometrical features that must be measured in the LABOR project as represented in Fig. 13.

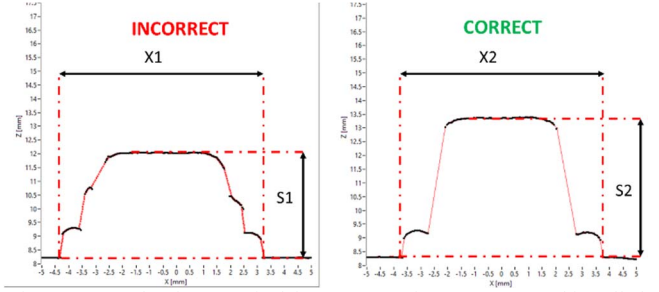


Fig. 13. Example of geometrical feature extraction on a corrected installed and defected fastener sleeve

Finally, a validation of the 2D Smart Inspection Tool measurement is given. A sample with four countersink hole has been prepared. Some defects and irregularities on the hole edge were present in order to test the Inspection Tool measurement algorithm robustness. The sample is presented in Fig. 14.



Fig. 14. Countersink hole sample

Each hole has been measured with the 2D Smart Inspection Tool (50 times) and with a CMM (coordinate measuring machine) "ZEISS O-INSPECT" as reference. In Fig. 15 and Fig. 16 results are shown for the internal and external diameters of each hole.

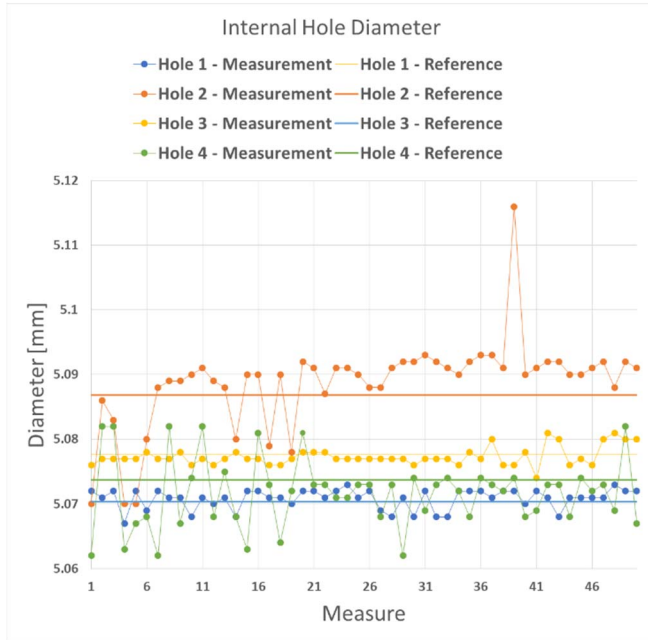


Fig. 15. Internal hole diameter measured with 2D Smart Inspection Tool

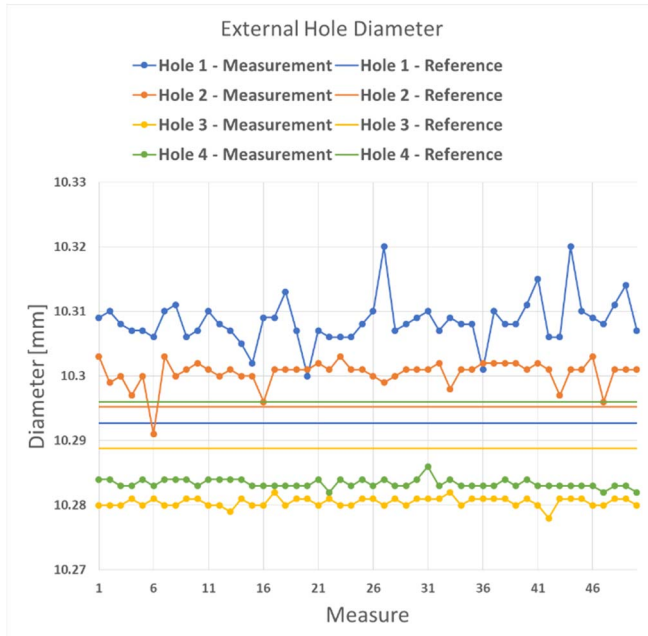


Fig. 16. External countersink hole diameter measured with 2D Smart Inspection Tool

Data has been analyzed and results are shown in TABLE II. For each hole, for both internal and external diameters, the measurement repeatability has been calculated and also the maximum deviation between the mean value and the true value from the CMM machine is given. Finally, the maximum repeatability values for all four holes are shown.

TABLE II. 2D Smart Inspection Tool Repeatability

TRUE VALUE from ZEISS O-INSPECT [mm]							
Hole 1		Hole 2		Hole 3		Hole 4	
INT	EXT	INT	EXT	INT	EXT	INT	EXT
5.1139	10.258	5.1105	10.251	5.127	10.257	5.1178	10.255
TRUE VALUE - MEAN VALUE [mm]							
Hole 1		Hole 2		Hole 3		Hole 4	
INT	EXT	INT	EXT	INT	EXT	INT	EXT
-0.042	0.0252	-0.033	0.0295	0.038	0.0431	-0.047	0.0536
REPEATABILITY (MAX VALUE - MIN VALUE) [mm]							
Hole 1		Hole 2		Hole 3		Hole 4	
INT	EXT	INT	EXT	INT	EXT	INT	EXT
0.02	0.004	0.007	0.004	0.046	0.012	0.006	0.02
MAX. REPEATABILITY INTERNAL DIAM. [mm]							
							0.046
MAX. REPEATABILITY EXTERNAL DIAM. [mm]							
							0.02

The results show, globally, good values for repeatability, better for the external diameter rather than the internal one. Data also show an offset between true values and measured values. The main reason for this offset can be a not precise alignment between the optical axis and the perpendicular of the target surface. This issue will be solved in the final system setup because the 2D Inspection Tool will be installed on the robot wrist that will be equipped with a normality sensor that will check and correct the correct orientation of the Inspection Tool prior to performing the measurement.

In Fig. 17 and Fig. 18 the measurements obtained with the 3D smart Inspection Tool are reported. A sample of four installed fasteners (Fig. 19) has been measured 50 times and, for each measurement, the mean value and the standard deviation have been evaluated. The graphs report, for each quantity, the maximum admissible value (in red) according to LABOR requirements (refer to TABLE I), the mean value and the standard deviation (in black). The five quantities evaluated are flushness (a), collar protrusion (b), stem protrusion (c), sleeve height (d) and sleeve diameter (e).

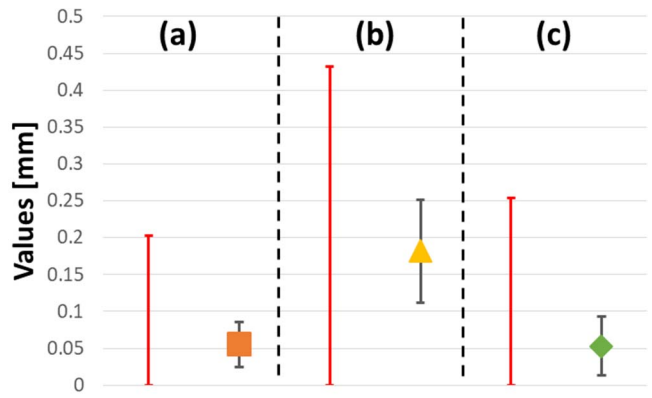


Fig. 17. 3D Smart Inspection Tool measurement results (1/2)

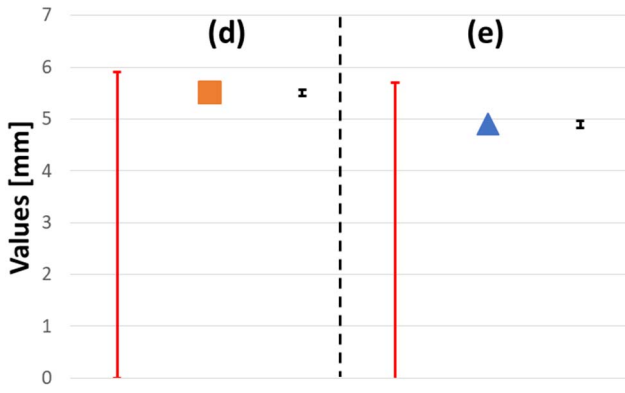


Fig. 18. 3D Smart Inspection Tool measurement results (2/2)

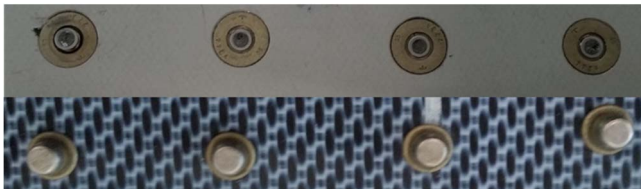


Fig. 19. Sample of installed fasteners

Also for the 3D Smart Inspection Tool, the results are positive and show that the proposed solution satisfies the project requirements. The obtained error is compatible with the required measurement accuracy. A detailed characterization of the proposed equipment will be presented in future works.

V. CONCLUSIONS

The Smart Inspection Tools presented in this paper satisfy the inspection requirements of the LABOR project and more in general the requirements usually applied in the aeronautical sector. Moreover, small dimensions and lightweight design have been guaranteed in order to mount the tools on small/medium scale robots. This is an important objective in order to pursue the automatization trend of the growing aircraft industry. In the followings, both tools will be installed on the LABOR robotic cell and thus performance on the real system will be tested and validated.

ACKNOWLEDGMENT

The research leading to these results has received funding from the European Commission H2020 Program – Clean Sky 2 JU, under GA n. 785419 LABOR - Lean robotized AssemBly and cOntrol of composite aeRostructures.

REFERENCES

- [1] Airbus, "Global Market Forecast (GMF) 2017-2036," Growing horizons, Apr. 2017.
- [2] S. Holt and R. Clauss, "Robotic drilling and countersinking on highly curved surfaces," SAE Technical Paper, 2015-01-2517, Sept. 2015.
- [3] <http://www.loxin2002.com/software>, [Accessed May 20, 2019].
- [4] <https://www.kuka.com/en-us/products/production-systems/aerospace-systems-engineering/material-handling-solutions/mobile-robotic-platform>, [Accessed May 20, 2019].
- [5] T. Dillhoefer, "Power RACe," SAE Technical Paper, 2017-01-2093, Sept. 2017.
- [6] www.labor-project.eu, European Community-Clean Sky 2 JU, [Accessed May 20, 2019].
- [7] D. Massa, M. Callegari, and C. Cristalli, "Manual guidance for industrial robot programming," *Industrial Robot: An International Journal*, vol. 42(5), pp. 457-465, 2015.
- [8] D. W. I. J. Meißner, M. S. F. Schmatz, D. I. F. Beuß, D. W. I. J. Sender, I. W. Flügge, and D. K. F. E. Gorr, "Smart human-robot-collaboration in mechanical joining processes," *Procedia Manufacturing*, vol. 24, pp. 264-270, 2018.
- [9] N. Jayaweera and P. Webb, "Automated assembly of fuselage skin panels," *Assembly Automation*, vol. 27(4), pp. 343-355, 2007.
- [10] M. B. Bauza, S. C. Woody, S. T. Smith, and R. J. Hocken, "Development of a rapid profilometer with an application to roundness gauging," *Precision engineering*, vol. 30(4), pp. 406-413, 2006.
- [11] Y. Chugui, L. Finogenov, V. Kiryanov, V. Nikitin, A. Sametov, and P. Zavyalov, "Inspection of holes parameters using a ring diffractive focuser," *VDI BERICHTE*, vol. 1844, pp. 433-444, 2004.
- [12] L. Pilny, L. De Chiffre, M. Piska, and M.F. Villumsen, "Hole quality and burr reduction in drilling aluminium sheets," *CIRP Journal of Manufacturing Science and Technology*, vol. 5(2), pp. 102-107, 2012.
- [13] Z. Usman, R.P. Monfared, N. Lohse, and M.R. Jackson, "An investigation of highly accurate and precise robotic hole measurements using non-contact devices," *International Journal of Metrology and Quality Engineering*, vol. 7(2), pp. 204, 2016.
- [14] N. Wu, W. Zhao, X. Wang, Y. Tao, and Z. Hou, "A novel design of through-hole depth on-machine optical measuring equipment for automatic drilling and riveting," *Applied Sciences*, vol. 8(12), pp. 2671, 2018.
- [15] E. Hong, H. Zhang, R. Katz, and J. S. Agapiou, "Non-contact inspection of internal threads of machined parts", *The International Journal of Advanced Manufacturing Technology*, vol. 62, pp. 221-229, Sept. 2011.
- [16] M. Baeg, S. Baeg, C. Moon, G. Jeong, H. Ahn, and D. Kim, "A new robotic 3D inspection system of automotive screw hole," *International Journal of Control, Automation, and Systems*, vol. 6 (5), pp. 740-745, Oct. 2008.
- [17] G. S. Spagnolo, L. Cozzella, and F. Leccese, "Viability of an optoelectronic system for real time roughness measurement," *Measurement*, vol. 58, pp. 537-543, 2014.
- [18] <http://8-tree.com> [Accessed May 20, 2019]
- [19] <http://www.unitedsciences.com/aeroscan> [Accessed May 20, 2019]
- [20] ISO 10360-7:2011 "Geometrical production specifications (GPS) - Acceptance and reverification tests for coordinate measuring machines (CMM) - Part 7: CMMs equipped with imaging probing systems", International Standard Organization, 2011.
- [21] G. Frankowsky, "Fast and contactless optical measurement of the 3D shape and surface roughness by projected micro fringes," *Proceedings of the XIth Int. Coll. on Surf.*, Germany (2004).